



## IDENTIFICATION OF THE CAUSATIVE AGENTS OF PROLIFERATIVE KIDNEY DISEASE IN *OREOCHROMIS NILOTICUS* AND *CLARIAS GARIEPINUS* USING PCR WITH SPECIAL REFERENCE TO THE ASSOCIATED HISTOPATHOLOGICAL ALTERATIONS

Eman I. Soror<sup>a</sup>, Karima F. Mahrous<sup>b</sup>, Ismail A.M.<sup>c</sup>, Amany A. Abbass<sup>a</sup>, Aziza, M.Hassan<sup>b</sup>

<sup>a</sup>Dept. Fish Diseases and Management, Fac. Vet. Med., Benha Univ., <sup>b</sup>Dept. Cell Biology, National Research Center, <sup>c</sup>Dept. Fish Diseases and Management, Fac. Vet. Med., Suez Canal Univ.

### ABSTRACT

In the present study, the causative agents of proliferative kidney disease (PKD) in both *Oreochromis niloticus* and *Clarias gariepinus* were identified based on the size and morphology of the spores and their polar capsules. The spores and polar capsules dimensions were measured by the Image J computer software. The occurrence of different myxosporean spores was confirmed by molecular biological technique using PCR with general and specific primers for different myxosporeans. Histopathological changes associated with PKD were recorded in both species. The results showed that there are 21 myxosporean species belonged to the genera *Myxobolus*, *Chloromyxum*, *Myxidium*, and *Triangula*. These include *Myxobolus sarigi*, *Myxobolus amieti*, *Myxobolus distichodi*, *Triangula* spp., *Myxobolus heterosporous type2*, *Myxobolus brachysporous*, *Myxobolus tilapiae*, *Myxobolus heterosporous type1*, *Myxobolus equatorialis*, *Myxobolus exigus*, *Myxobolus hydrocuni*, *Myxobolus* spp., *Myxobolus dossoui*, *Myxobolus heterosporous1*, *Myxidium* spp., *Chloromyxum* spp., *Sphaerospora* spp., *Tetracapsuloid tilapiae*, *Thelohanellus* spp., *Henneguya* spp., and *PKDX tissue form*. The PCR results showed bands at 1600 bp specific for *Myxobolus* spp., at 450 bp specific for *Chloromyxum* (*Tetracapsuloid* spp.), and at 1400 bp specific for *Sphaerospora* spp. in both *O. niloticus* and *C. gariepinus*. The general primer for Myxozoan produced bands at 1700 bp whereas Myxosporea specific but species unspecific primers produced bands at 900bp. Histopathological examination showed extrasporogonic stages of the parasite in the kidney interstitium surrounded by granulomatous inflammatory cell infiltration, while the sporogonic stages were observed intraluminal or within the epithelial cells of some renal tubules. Necrobiosis of epithelial lining renal tubules was seen in many affected kidney tissues. Proliferations of interstitial fibrous connective tissue with degeneration of the renal tubular epithelium were detected in some affected kidneys.

**KEY WORDS:** Histopathology, Morphology, Myxosporean, PCR, PKD.

(BVMJ-23 [1]: 159-170, 2012)

### 1. INTRODUCTION

In Egypt, proliferative kidney disease was observed to be epidemic among Tilapia fishes and known as Tilapia proliferative kidney disease (TPKD) [8]. The disease is characterized by a severe swelling of the kidney induced by the host immune response to the presence of extrasporogonic stages of a myxozoan parasite [4, 19, 30]. *Tetracapsuloid*

*bryosalmonae* parasitizes a broad range of freshwater bryozoans hosts, some of which occur throughout the holarctic [29, 37]. Recent genetic studies providing evidence for ongoing gene flow among bryozoans population point to migratory water fowl as agents of occasional long distance dissemination with bryozoans dispersive stages (statoplasts) [13]. In this study, the

causative agents of proliferative kidney disease (PKD) in both *O. niloticus* and *C. gariepinus* were identified based on the size and morphology of the spores and their polar capsules. The spores and polar capsules dimensions were measured by the Image G computer software. The occurrence of different Myxosporean spores was confirmed by molecular biological technique using PCR with general and specific primers for different Myxosporeans. Histopathological changes associated with PKD were recorded in both species.

## 2. MATERIAL AND METHODS

### 2.1. Fishes

This study used 500 fish, of which 266 were *O. niloticus* with average weight of 120±10 g and 234 *C. gariepinus* with average weight of 200±15g obtained from El-Riah El-Tawfiki and its tributaries.

### 2.2. Microscopic examinations of kidney preparations.

Specimens from examined kidneys and nodules if present with few drops of saline were squashed and examined under

microscope. The spores were examined for identification and taxonomical classification as previously described [22, 23] and using the keys to genera and species of myxosporea in Africa [12].

### 2.3. Classification of the causative agents based on the size and morphology.

Images were captured by Sony digital camera from different microscopical fields containing the spores. These images were imported to the Image J program for measuring the dimensions of every type of spores and the polar capsules and the results were exported to excel file [1].

### 2.4. The polymerase chain reaction (PCR).

Kidney samples from the infected fish were excised and frozen at -20 °C for PCR analysis [22]. Commercial DNA extraction kit (purchased Promega Corporation, Madison, WI, USA) for genomic DNA extraction from collected kidney samples. The Kit include: Nuclei lysis solution, RNase solution and protein precipitation solution. Specific primers were used for identification of the causative agents (purchased from Eurofins MWG /Operon). Six types of primers were used follow:

Primer	NAME	Sequence	Reference
Any myxozoan	18e	5'-TGG TTG ATC CTG CCA GT-3'	Hillis and Dixon [16]
	18g	5'-GGT AGT AGC GAC GGG CGG TGT G-3'	
	Myxgp2F	5'-TGG ATA ACC GTG GGAAA-3'	Kent <i>et al.</i> [21]
<i>Tetracapsuloid bryosalmonae</i>	Act1R	5'-AATTTACCTCTCGCTGCCA-3'	Kent <i>et al.</i> [21]
	5F	5'-CCTATCAATGAGTAGGAGA-3'	
Myxobolus spp.	6R	5'GGACCTTACTCGTTTCCGACC-3'	Hillis and Dixon [16] Whipps <i>et al.</i> [35] Andree <i>et al.</i> [3]
	18e	5'-CTGGTTGATTCTGCCAGT-3'	
	18r	5'-CTACGGAAACCTTGTTAC-3'	
	MX5	5'CTGCGGACGGCTCAGTAAATCAGT-3'	
	MX3	5'CCAGGACATCTTAGGGCATCACAGA-3'	
Sphaerospora spp.	SphF	5'ACTCGTTGGTAAGGTAGTGGCT-3'	Eszerbauer and Szekely [24]
	SphR	5'-GTTACCATTGTAGCGCGCGT-3'	

The PCR reaction for 18e, 18g, Myxgp2F, Act1R, 5F, and 6R was performed in 25ul volumes with 0.2 units of Titanium Taq DNA polymerase and 10x buffer containing 1.5mM MgCl<sub>2</sub>, 0.2 mM of each dNTP, 0.5Mm of each primer and 1 µl of template. Denaturation of DNA (95°C for 3 minutes) was followed by 30 cycles of amplification 95°C for 50 sec, annealing

temperature (63°C for 18e and 18g, 58°C for Myxgp2F and Act1R and 55°C for 5F and 6R) for 50 sec., and 70°C for 1 min 20 sec and terminated by 4 min extension (70°C). PCR products were separated in 1% agarose gel containing ethidium bromide in sodium boric acid buffer at 300v for 15 min. and there after visualized under UV light. The PCR reaction for 18e,

18r, MX5, MX3, and SphF, and SphR in the following conditions: genomic DNA was amplified with the primer pair 18e and 18r. The total volume of the PCR reaction was 25ul which contained approximately 5 to 25 ng DNA, 0.5x Taq PCR reaction buffer, 1.5 mM Mgcl<sub>2</sub>, 0.2mM dNTP mix, 0.5 mM of each primer, and 2u of Taq DNA polymerase. Amplification condition were 95°C for 50 sec, 58°C for 50 sec, and 72°C for 80 sec for 35 cycles, with a terminal extension at 72°C for 7 min, when a weak band was detected on 1% agarose gel in TBE buffer, the amplification was followed by nested PCR assay with inner primer pairs MX5 and MX3. The cycling condition with the primers MX5 and MX3 were 95°C for 30 sec, 50°C for 30 sec, and 72°C for 60 sec for 35 cycles, and were terminated with an extension period at 72°C for 7 min. For the primers SphF and SphR the amplification conditions were 95°C for 50 sec, 56°C for 50 sec and 72°C for 80 sec for 35 cycles, with a terminal extension at 72°C for 7 min. PCR products were electrophoresed in 1% agarose gel stained with ethidium bromide.

### 2.5. Histopathological examination.

Tissue specimens of kidneys and urinary bladder were fixed in 10% neutral buffered formalin (NBF) then dehydrated and blocked in paraffin wax. Tissue sections of 5-7 microns thickness were stained with Haematoxylin and Eosin [6].

## 3. RESULTS

### 3.1. Identification of different types of myxosporean spores

As shown in Fig. 1 and Table 1, there were at least 21 myxosporean species belonged to the genera *Myxobolus*, *Chloromyxum*, *Myxidium*, and *Triangula*. These include *Myxobolus sarigi*, *Myxobolus amieti*, *Myxobolus distichodi*, *Triangula* spp., *Myxobolus heterosporous type2*, *Myxobolus brachysporous*, *Myxobolus tilapiae*, *Myxobolus heterosporous type1*,

*Myxobolus equatorialis*, *Myxobolus exigus*, *Myxobolus hydrocuni*, *Myxobolus* spp., *Myxobolus dossoui*, *Myxobolus heterosporous1*, *Myxidium* spp., *Chloromyxum* spp., *Sphaerospora* spp., *Tetracapsuloid tilapiae*, *Thelohanellus* spp., *Henneguya* spp., and *PKDX tissue form*.

### 3.2. The results of PCR

The PCR amplification of DNA obtained from the kidney tissues of *O. niloticus* and *C. gariepinus* affected with PKD (previously proven microscopically to be infested with different types of Myxosprea) showed different PCR products related to various species of *Myxobolous*, *Sphaerospora*, *Tetracapsuloid* species.

In *O. niloticus*, the PCR amplification performed using primer (18e-18g) that can be used for identification of Myxozoan produced bands at 1700 bp (Fig. 2). The PCR results were confirmed by nested PCR with *Myxosprea* primers (*MyxgF-ActR*) and the bands of the expected size (900bp) were obtained for both of them in all samples (Fig.3). For *Myxobolous* species primer (18e-18r), the bands of the expected size (2000 bp) appeared (Fig. 4) and the nested PCR performed for weak or faint bands with MX5-MX3 at 1600 bp (Fig. 5) and SphF-SphR primers at 1400 bp (Fig.6). PCR amplification performed on the DNA with *Sphaerospora* species primer showed bands at 1400 bp (Fig. 7). Also, the *Tetracapsuloid* species primer produced bands at 450 bp (Fig. 8).

In *C. gariepinus*, the result of PCR performed using 18e-18g primer (*Myxozoan*) showed bands at 1700 bp (Fig. 9). Nested PCR using *MyxgF-ActR* primer (*Myxosporea*) demonstrated the product at 900 bp (Fig. 10). PCR using primer 18e-18r showed bands at 2000 bp (Fig. 11). The nested PCR applied on the weak and faint bands using MX5-MX3 primer (*Myxobolous* species) and SphF-SphR primer (*sphaerospora* species) produced bands at 1600, 1400 bp (Fig. 5, 12).

Table 1 Morphology and dimensions of the spores and polar capsules identified by microscopic examination.

No	Species	Spore shape	Polar capsule shape	Spore length (µm)	Spore width (µm)	Polar capsule Length (µm)	Polar capsule width (µm)	Host
1.	Myxobolus sarigi	triangular to subspherical	spherical and equal	15.7625	12.675	5.0375	4.0625	<i>O. niloticus</i> <i>C.gariepinus</i>
2.	Myxobolus amieti	Pyriiform	large and elongated polar	16.0875	9.425	9.9125	3.0875	<i>O. niloticus</i> <i>C.gariepinus</i>
3.	Myxobolus distichodi	Pyriiform	Flask	15.1125	8.125	4.55	2.275	<i>O. niloticus</i> <i>C.gariepinus</i>
4.	Triangula spp.	Rounded, triangular	Subspherical	12.8375	11.2125	4.3875	3.7375	<i>O. niloticus</i>
5.	Myxobolus heterosporous type2	Ovoid to pyriform	Flask	13.975	8.9375	7.6375	2.275	<i>O. niloticus</i> <i>C.gariepinus</i>
6.	Myxobolus brachysporous	Ellipsoidal	Ovoid	15.275	9.2625	5.0375	3.7375	<i>O. niloticus</i> <i>C.gariepinus</i>
7.	Myxobolus tilapiae	Ovoid	Ovoid	17.0625	11.05	3.575	2.275	<i>O. niloticus</i>
8.	Myxobolus heterosporous type1	ovoid to pyriform	Pyriiform	16.4125	10.725	4.3875	2.7625	<i>C.gariepinus</i>
9.	Myxobolus.equatorialis	Pyriiform	Rounded	13.975	6.0125	2.7625	1.7875	<i>O. niloticus</i>
10.	Myxobolus exigus	Round	Oval	8.6125	7.9625	3.9	2.275	<i>C.gariepinus</i>
11.	Myxobolus hydrocuni	Ovoid to pyriform	Flask	13.65	7.6375	7.475	2.275	<i>O. niloticus</i>
12.	Myxobolus spp.	Rounded	Ovoid	6.3375	7.6375	2.4375	2.275	<i>C.gariepinus</i>
13.	Sphaerospora spp.	ovoid to pyriform	Flask	11.05	10.4	4.875	2.1125	<i>O. niloticus</i>
14.	Myxobolus heterosporous	Ellipsoidal	Ovoid	18.525	11.5375	5.525	2.6	<i>C.gariepinus</i>
15.	Myxidium spp	Fusiform or ellipsoidal	pyriiform or spherical	18.5	6.7	4.2	3.9	<i>O. niloticus</i> <i>C.gariepinus</i>
16.	Chloromyxum spp1	Rounded to triangular	Ovoid (3 polar capsules)	13.2	12.8	3.4	2.6	<i>O. niloticus</i>
17.	Sphaerospora spp.	Spherical or subspherical	rounded	7.8	7.6	2.5	2.8	<i>C.gariepinus</i>
18.	Tetracapsuloid tilapiae in Urinary bladder	Rounded to triangular	Ovoid (4 polar capsules)	12.9	12.4	2.9	2.7	<i>O. niloticus</i>
19.	Thelohanelius spp.	Ovoid	Single ovoid at one end	10.1	7.8	3.1	2.9	<i>O. niloticus</i>
20.	Henneguya spp.	Fusiform	Pyriiform	15.275	10.4	4.875	2.925	<i>C.gariepinus</i>
21.	PKDX tissue form	Subspherial	spherical	12.01	9.1	3.5	3.4	<i>O. niloticus</i> <i>C.gariepinus</i>

Also the PCR performed by using Sphaerospora primer and Tetracapsuloid species primers produced bands at 1400 and 450 bp, respectively (Fig. 13, 14).

### 3.3. The histopathological examination

The microscopical examination of fish infected with PKD revealed chronic granulomatous interstitial inflammatory response of the kidneys, accompanied by limited destruction of some renal tubules. Diffusely, the cortical and medullary interstitium were expanded by clusters of mononuclear inflammatory cells mainly macrophages, lymphocytes and eosinophilic granular cells. Moreover, circumscribed granuloma replaced large

area of renal tissue, and composed of central necrosis and mineralization with aggregates of epithelioid and mononuclear cells and rimmed by fibrous tissue capsule was rarely observed. The lining epithelium of the proximal and distal convoluted tubules exhibited degenerative and necrotic changes.

The degenerated epithelium was either swollen with pale vacuolated cytoplasm, or filled with variable sizes hyalinized eosinophilic droplets that obscured the normal architecture of some renal tubules. The necrotic epithelium was shrunken, with hypereosinophilic cytoplasm and pyknotic nuclei, occasionally, the necrotic epithelium exfoliated in the lumen of

tubules in the form of cellular casts. Numerous extrasporogonic stages and primary cells contained one or more daughter cells of myxosporean parasites were found scattered in the interstitial tissue, haemopoietic tissue and in stroma of focal granuloma surrounded by macrophages and lymphocytes. The sporogonic stages of myxosporean parasites were observed intraluminal or within the epithelial cells of renal tubules. The fully formed spores were ovoid with indistinguishable valves and two spherical polar capsules at the anterior end (Fig. 15 A-F).

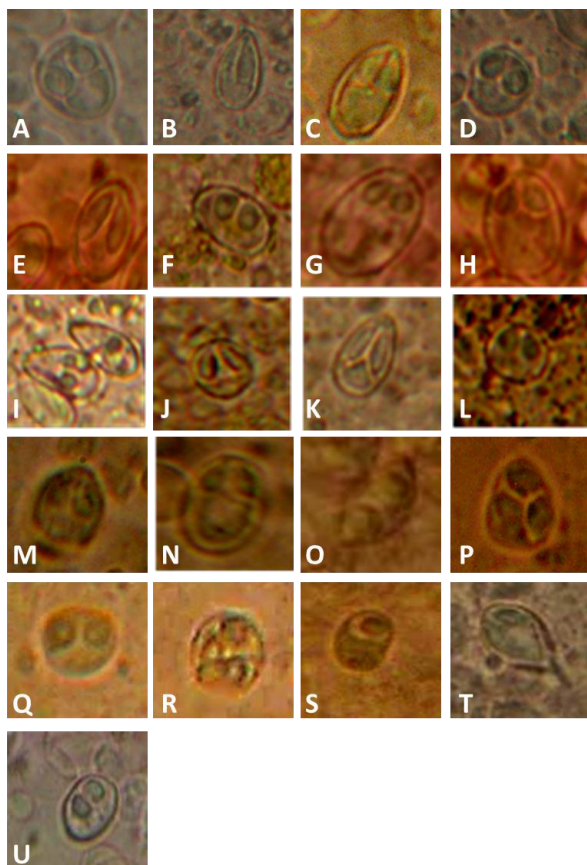


Fig. 1 Identification of different types of myxosporean spores: a-Myxobolus sarigi b-Myxobolus amieti c-Myxobolus distichodi d-Triangula spp e-Myxobolus heterosporous type2 f-Myxobolus brachysporous g-Myxobolus tilapiae h-Myxobolus heterosporous type1 i-Myxobolus equatorialis j- Myxobolus exigus k-Myxobolus hydrocuni l-Myxobolus spp m-sphaerospora spp in tissue n-Myxobolus heterosporous o-Myxidium spp p-Chloromyxum spp1 q- Sphaerospora spp r-tetracapsuloid tilapiae in Urinary bladder s-Thelohanellus spp. t-Henneguya spp. u- PKDX tissue form.

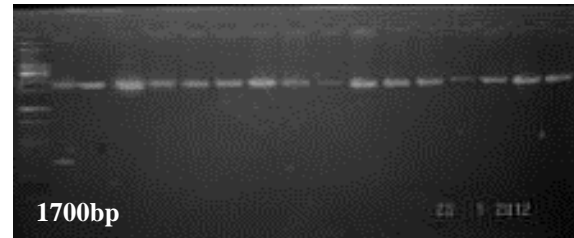


Fig. 2 Ethidium bromide-stained gel of amplified PCR products representing amplification of 18e-18g gene (myxozoan) in Oreochromis niloticus. Lane 1: 2000-bp ladder marker. Lanes: 2–17: 1700-bp PCR products amplified from Oreochromis niloticus DNA

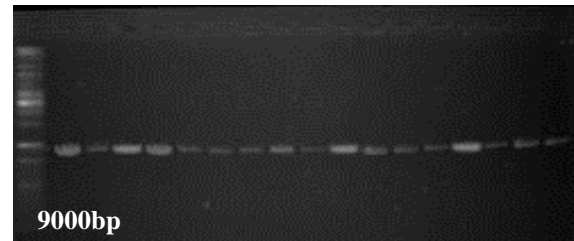


Fig. 3. Ethidium bromide-stained gel of nested PCR products representing amplification of MyxgF-ActR gene (myxosporea) in Oreochromis niloticus. Lane 1: 2000-bp ladder marker. Lanes: 2–18: 900-bp PCR products amplified from Oreochromis niloticus DNA.

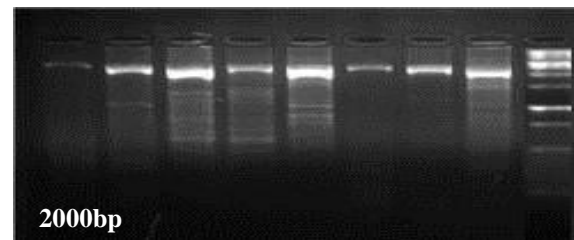


Fig. 4. Ethidium bromide-stained gel of amplified PCR products representing amplification of 18e-18r gene (myxobolus) in Oreochromis niloticus. Lane 1: 2000-bp ladder marker. Lanes: 2–8: 2000-bp PCR products amplified from Oreochromis niloticus DNA.



Fig. 5. Ethidium bromide-stained gel of nested PCR products representing amplification of MX5-MX3 gene (myxobolus) in Oreochromis niloticus and Clarias gariepinus. Lane 1: 2000-bp ladder marker. Lanes: 2,3,4,7 and 8: 1600-bp PCR products amplified from Oreochromis niloticus DNA. Lanes: 10,11,14,15 and 16: 1600-bp PCR products amplified from Clarias gariepinus DNA.

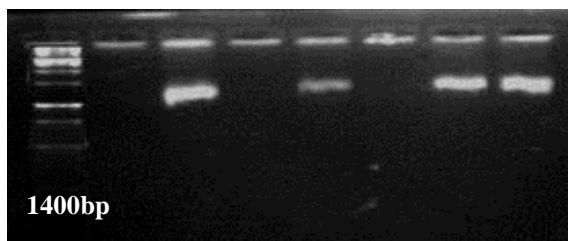


Fig. 6. Ethidium bromide-stained gel of nested PCR products representing amplification of SphF-SphR gene (*Sphaerospora*) in *Oreochromis niloticus*. Lane 1: 2000-bp ladder marker. Lanes: 3,5,7, and 8: 1400-bp PCR products amplified from *Oreochromis niloticus* DNA.

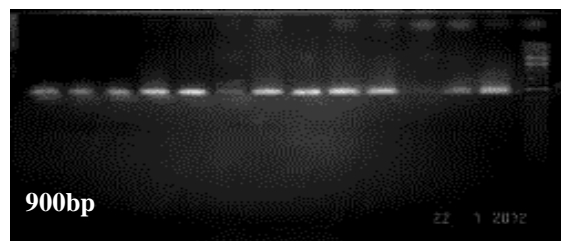


Fig. 10. Ethidium bromide-stained gel of nested PCR products representing amplification of MyxgF-ActR gene (*myxosporea*) in *Clarias gariepinus*. Lane 1: 2000-bp ladder marker. Lanes: 2-18: 900-bp PCR products amplified from *Clarias gariepinus* DNA.

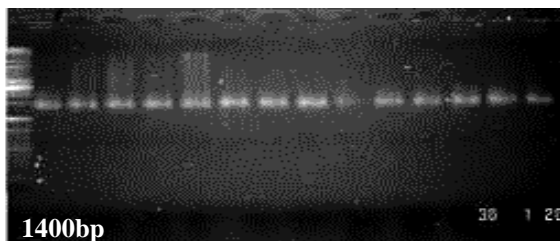


Fig. 7 Ethidium bromide-stained gel of amplified PCR products representing amplification of SphF-SphR gene (*Sphaerospora*) in *Oreochromis niloticus*. Lane 1: 2000-bp ladder marker. Lanes: 2-15: 1400-bp PCR products amplified from *Oreochromis niloticus* DNA.

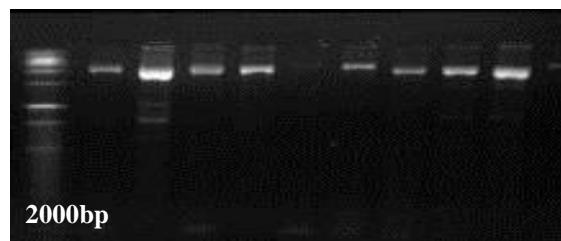


Fig. 11. Ethidium bromide-stained gel of amplified PCR products representing amplification of 18e-18r gene (*Myxobolus*) in *Clarias gariepinus*. Lane 1: 2000-bp ladder marker. Lanes: 2-11: 2000-bp PCR products amplified from *Clarias gariepinus* DNA.

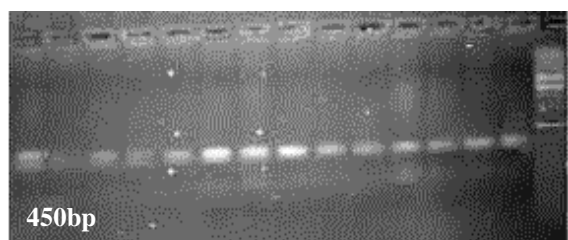


Fig. 8. Ethidium bromide-stained gel of amplified PCR products representing amplification of 5F-6R gene for *Tetracapsuloid bryosalmonae* in *Oreochromis niloticus*. Lane 1: 2000-bp ladder marker. Lanes: 2-15: 450-bp PCR products amplified from *Oreochromis niloticus* DNA.

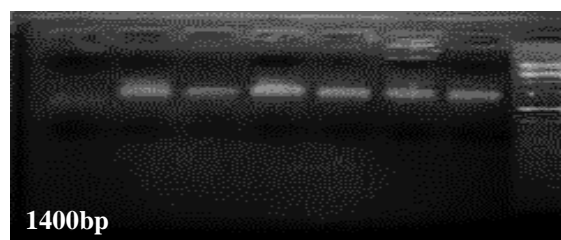


Fig. 12. Ethidium bromide-stained gel of nested PCR products representing amplification of SphF-SphR gene (*Sphaerospora*) in *Clarias gariepinus*. Lane 1: 2000-bp ladder marker. Lanes: 2-8: 1400-bp PCR products amplified from *Clarias gariepinus* DNA.

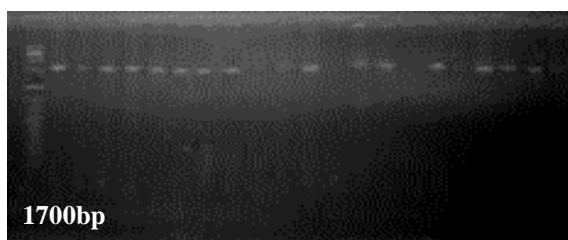


Fig. 9. Ethidium bromide-stained gel of amplified PCR products representing amplification of 18e-18g gene (*myxozoan*) in *Clarias gariepinus*. Lane 1: 2000-bp ladder marker. Lanes: 2-22: 1700-bp PCR products amplified from *Clarias gariepinus* DNA.

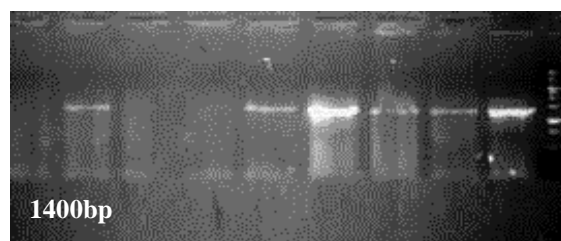


Fig. 13. Ethidium bromide-stained gel of PCR products representing amplification of SphF-SphR gene (*Sphaerospora*) in *Clarias gariepinus*. Lane 1: 2000-bp ladder marker. Lanes: 2-9: 1400-bp PCR products amplified from *Clarias gariepinus* DNA.

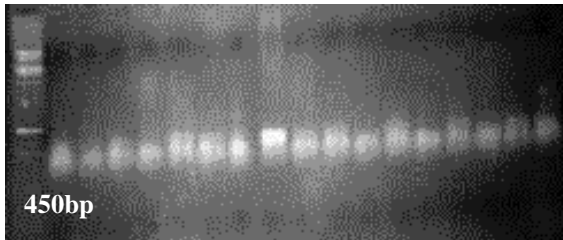


Fig. 14. Ethidium bromide-stained gel of amplified PCR products representing amplification of 5F-6R gene for *Tetracapsuloid bryosalmonae* in *Clarias gariepinus*. Lane 1: 2000-bp ladder marker. Lanes: 2–18: 450-bp PCR products amplified from *Clarias gariepinus* DNA.

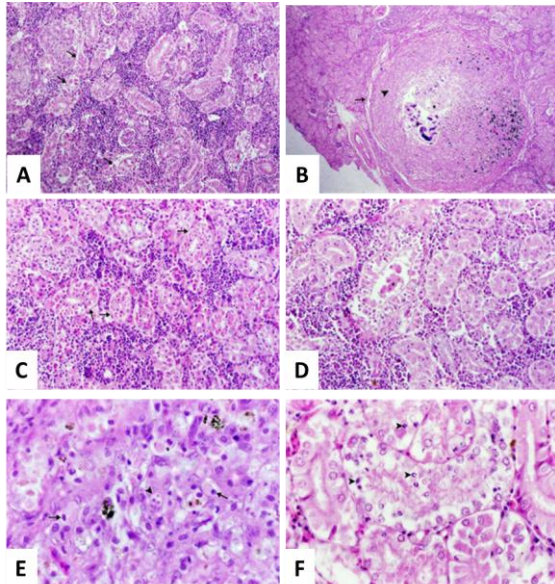


Fig15. (A-F) A. Kidney tissue infected with PKD showing chronic granulomatous interstitial inflammatory response (asterisk) accompanied by limited destruction of some renal tubules (arrow). B. Kidney tissue infected with PKD showing circumscribed granuloma replaced large area of renal tissue, and composed of central necrosis and mineralization (asterisk) with aggregates of epithelioid and mononuclear cells (arrow head) and rimmed by fibrous tissue capsule (arrow). H&E stain x 100. C. Kidney tissue infected with PKD showing hyaline droplet degeneration obscured the normal architecture of some renal tubules (arrow). H&E stain x 400. D. Kidney tissue infected with PKD showing cellular casts (asterisk) in the lumen of the necrotic tubules. H&E stain x 400. E. Kidney tissue infected with PKD showing extrasporogonic stages (arrow) and primary cells contained one or more daughter cells (arrow head) of myxosporean parasites in the stroma of focal granuloma surrounded by macrophages and lymphocytes. H&E stain x 1000. F. Kidney tissue infected with PKD showing sporogonic stages (arrow head) of myxosporean parasites within the epithelial cells of renal tubules H&E stain x 1000.

#### 4. DISCUSSION

In this study, different types of mature myxosporean spores were identified by microscopical examination of the fresh

preparations of affected kidneys. Similar results were recorded by El-Mansy and Abdel-Ghaffar [8]. They identified seventeen myxosporean species belong to the genera *Myxobolus*, *Triangula* and *Chloromyxum* in tilapia fishes from the River Nile at El-Rahawy drain. The Presence of different myxosporean spores together in the kidney of almost all examined tilapia fishes could be attributed to two reasons, first that mature spores may come from their specific organs to the kidney via blood and in this case the kidney infection could be used as a diagnostic evidence for the presence of myxosporean parasites and the other reason that some spores may originate as a final stage of the development of PKD cells within the kidney tissues because mature spores were already found together with these stages surrounded with cyst like structures [8].

The spores have different sizes and morphology. Spores were identified according to the shape and dimension (length-width) and the polar capsule shape and dimension using the keys to genera and species of Myxosporea in Africa [12]. The main species identified according to this method were belonged to the genera *Myxobolus*, *Chloromyxum*, *Myxidium*, and *Triangula*. Twenty one 21 species were identified as *Myxobolus sarigi*, *Myxobolus amieti*, *Myxobolus distichodi*, *Triangula* spp., *Myxobolus heterosporous type2*, *Myxobolus brachysporous*, *Myxobolus tilapiae*, *Myxobolus heterosporous type1*, *Myxobolus equatorialis*, *Myxobolus exigus*, *Myxobolus hydrocuni*, *Myxobolus* spp., *Myxobolus dossoui*, *Myxobolus heterosporous1*, *Myxidium* spp., *Chloromyxum* spp., *Sphaerospora* spp., *Tetracapsuloid tilapiae*, *Thelohanellus* spp., *Henneguya* spp., and *PKDX tissue form*.

The PCR was used as a confirmatory tool for the diagnosis of different types of Myxosporeans associated with PKD in *O. niloticus* and *C. gariepinus*. The PCR

amplification of DNA obtained from the kidney tissues of *O. niloticus* and *C. gariepinus* affected with PKD (previously proven microscopically to be infested with different types of myxosporea) showed different PCR products related to various species of Myxobolous, Sphaerospora, Tetracapsuloid.

In *O. niloticus*, the PCR amplification performed using the primer (18e-18g) that can be used for identification of Myxozoan produced bands at 1700 bp. Because this primer can identify any type of Myxozoans, it was followed by nested PCR using more specific primers but species unspecific (MyxgF- ActR). This primer demonstrated bands at 900bp in all samples. To identify different types of Myxosporea, species specific primers were used. Myxobolous species primer (18e-18r) produced the bands at 2000 bp. These findings were similar to those obtained by Molnár *et al.* [26]. The nested PCR performed for weak or faint bands with MX5-MX3 at 1600 bp. This finding was also coincided with Molnár *et al.* [26]. The use of SphF-SphR primers on nested PCR produced bands at 1400 bp, confirming the presence of Sphaerospora species in kidneys of *O. niloticus* affected with PKD. The same results were also obtained when performed on the DNA with Sphaerospora species primer. Similar PCR findings were recorded by Eszterbauer and Szekely [10]. *Tetracapsuloid bryosalmonae* primer produced bands at 450 bp. This result confirms the role of *Tetracapsuloid bryosalmonae* in the pathogenesis of PKD in *O. niloticus*. Similar PCR observation was recorded by Holzer *et al.* [17].

In *C. gariepinus*, the result of PCR performed using 18e-18g primer (Myxozoan primer) showed bands at 1700 bp. The nested PCR using MyxgF-ActR primer (Myxosporea) demonstrated the product at 900 bp. PCR using Myxobolous species primer 18e-18r showed bands at 2000 bp. The nested PCR applied on the weak and faint bands using MX5-MX3 primer (Myxobolous species) produced

bands at 1600 bp. These findings were similar to those obtained by Molnár *et al.* [26], and confirm the implication of Myxobolous spp. in etiology of PKD in *C. gariepinus*. PCR amplification using SphF-SphR primer produced bands at 1400 bp confirming the occurrence of Sphaerospora species as one of the causative agent of PKD in *C. gariepinus*. Similar PCR findings were recorded by Eszterbauer and Szekely [10]. PCR performed by using *Tetracapsuloid bryosalmonae* primers produced bands at 450 bp. This result confirms that *Tetracapsuloid bryosalmonae* is one of the causative agents of PKD in *C. gariepinus*. Similar PCR finding was observed by Holzer *et al.* [17].

Histopathological examination using H&E of kidney tissue of fish affected with PKD showed chronic inflammation of the kidney and the tissue sections revealed the protozoan primarily in the kidney interstitium associated with a granulomatous interstitial nephritis and tubular atrophy. These findings agree with those recorded by previous authors [4, 5, 14, 20, 36].

Histological finding in some affected fish showed hyper cellularity of the kidney interstitium due to mononuclear cell proliferation and infiltration associated with the parasites and the infected fish exhibited a reduced number of tubules. Parasites may be surrounded by macrophages and lymphocytes and in most fishes found hypertrophied kidney with developing myxosporean spores as evidenced by polar capsule formation were observed. The intraluminal organisms appeared as myxosporean trophozoites due to formation of multicellular spores with polar capsules. These histopathological findings were nearly similar to those observed by earlier authors [8, 9, 11, 25, 27, 33 34]. The hyperplastic response of lymphoid tissue associated with proliferative kidney disease could be attributed to the immunopathological condition mediated by the host leukocytes



and macrophages which are the principal actors in these conditions [24].

The extrasporogenic stages of the parasite were observed in the kidney interstitium surrounded by granulomatous inflammatory cell infiltration appeared as major histopathological changes. Necrobiosis of epithelial lining renal tubules was observed in many affected tissues. Proliferation of interstitial fibrous connective tissue with vacuolization of the renal tubular epithelium occurs in some affected kidneys. These histopathological findings were nearly similar to those reported by previous authors [25, 27, 31].

In a conclusion, the results demonstrated that PKD in *O. niloticus* and *C. gariepinus* is caused by different types of myxosporean spores belong to Myxobolus, Sphaerospora, Myxidium, Triangula, Chloramyxum and *Tetracapsuloid bryosalmonae*. At least 21 species were identified. The PKD caused by these species adversely affects the kidneys by hyperplasia of lymphocyte-macrophage cells and reduction of the functional nephrons.

## 5. REFERENCES

1. Abramoff, M.D., Magelhaes, P.J. and Ram, S.J. 2004. Image processing with Image J. *Biophoton. Int.* **11**: 36-42
2. Anderson C., Canning E.U. and Okamura B. 1999. 18S rDNA sequences indicate that PKX organism parasitizes Bryozoa. *Bull. Eur. Ass. Fish Path.* **19**: 94–97.
3. Andree, K.B., Szely, C., Molnar, K., Gresoveic, S.G. and Hedrick, R.P. 1999. Relationships among members of the genus myxobolus (Myxozoa: bivalvidae) based on small subunit ribosomal RNA sequences. *J. parasitol.* **58**: 68-74.
4. Chilmonczyk S, Monge D, De Kinkelin P 2002. Proliferative kidney disease: cellular aspects of the rainbow trout, *Oncorhynchus mykiss* (Walbaum), response to parasitic infection. *J Fish Dis* **25**: 217–226
5. Clifton-Hadley, R.S., Feist, S.W. 1989. Proliferative kidney disease in brown trout *Salmo trutta*: further evidence of a myxosporean aetiology. *Dis Aquat Org* **6**: 99–103
6. Drury, B.A.R. and Wallington, A.E. 1980. Carleton's histological technique, 5th. Ed. Oxford, NY. Toronto. Oxford Univ. Press
7. Eissa, A.E., Abu Mourad, I.M.K. and Borhan T. 2006. A contribution on myxosoma Infection in Cultured *Oreochromis niloticus* in Lower Egypt. *Nature and Science* **4**: 40-46.
8. El-Mansy, A. and Abdel-Ghaffar, F. 2003. Tilapian proliferative kidney disease (TPKD) and a diagnostic evidence for the presence of myxosporean parasites. *J. Egypt. Ger. Soc. Zool.* **40D**: 139-159.
9. El-Matbouli, M. and Hoffman, R.W. 2002. Influence of water quality on the outbreak of proliferative kidney disease: field studies and exposure experiments. *J. Fish Dis.* **25**: 459–467.
10. Eszterbauer, E. and Szekely, C. 2004. Molecular phylogeny of the kidney parasitic *Sphaerospora renicola* from common carp (*Cyprinus caprio*) and *Sphaerospora* species from Gold fish (*Carassius auratus auratus*). *Acta. Vet Hung* **52**: 469-478.
11. Feist, S. W., Peeler, E. J., Gardiner, R., Smith, E. and Longshaw, M. 2002. Proliferative kidney disease and renal myxosporidiosis in juvenile salmonids from rivers in England and Wales. *J. Fish Dis.* **25**: 451–458.
12. Fomena, A and Bouix, J. 1997. Myxosporea (protozoa: myxozoon) of freshwater fishes in Africa: keys to genera and species. *Cyst. Parasitol.* **37**: 161-178.
13. Freeland, J.R., Noble, L.R. and Okamura, B. 2000. Genetic consequences of the metapopulation biology of a facultatively sexual freshwater invertebrate. *J. Evol. Biol.* **13**: 383– 395.
14. Hedrick R.P., MacConnell E. and de Kinkelin P. 1993. Proliferative kidney disease of salmonid fish. In: Annual Review of Fish Diseases 3 (ed. by M. Faisal & F. M. Hetrick). Elsevier Sciences, Oxford. Pp.277–290.
15. Henderson, M. and Okamura, B. 2004. The phylogeography of salmonid proliferative kidney disease in Europe and North America. *Proc. R. Soc. Lond. B* **271**: 1729–1736.
16. Hillis, D.M. and Dixon, M.T. 1991. Ribosomal DNA: molecular evolution and

- phylogentic inference. *Q. Rev. Biol.* **66**: 411-453.
17. Holzer, A.S., Sommerville, C. and Wootten, R. 2006. Molecular relationships and phylogeny in a community of myxosporeans and actinosporeans based on their 18S rDNA sequences. *Int. J. Parasitol.* **34**: 1099-1111.
  18. Kent M.L. and Hedrick R.P. 1986. Development of the PKX myxosporean in rainbow trout *salmo gairdneri*. *Dis. Aquat. Org.* **1**: 169-182.
  19. Kent, M.L., Khattra, J., Hedrick, R.P. and Devlin, R.H. 2000. *Tetracapsula renicola* n. sp. (Myxozoa: Saccosporidae), the PKX myxozoan-the cause of proliferative kidney disease of salmonid fishes. *J Parasitol* **86**:103–111
  20. Kent, M.L, Margolis, L. and Corliss, JO 1994. The demise of a class of protists: taxonomic and nomenclatural revisions proposed for the protist phylum Myxozoa Grasse, 1970. *Can J Zool* **72**: 932– 937
  21. Kent, M.L., Khattra, J., Hervio, D.M.L. and Devlin, R.H. 1998. Ribosomal DNA sequence analysis of isolates of the PKX myxosporean and their relationship to members of the genus *Sphaerospora*. *J. Aquat. Anim. Health* **10**: 12–21.
  22. Levine, N.D., Corliss, J.O., Cox, F.E.G., Deroux, G., Grain, J., Honigberg, B.M., Leedale, J.F., Loeblich, A.R., Lom, J., Lynn, D., Merinfeld, E.G., Page, F.C., Polgansky, G., Sprague, V., Favara, J. and Wallace, F.G. 1980. A newly revised classification of the protozoa. *J. protozoan* **27**: 37-58.
  23. Lom, J. and Nobble, E.R. 1984. Revised classification of the class Myxosporean butschli, 1981. *Folia parasitol.* **31**: 193-205.
  24. MacConnell, E., Smith, C.E., Hedrick, R.P. and Speer, C.A. 1989. Cellular inflammatory response of rainbow trout to the protozoan parasite that causes proliferative kidney disease. *J. Aquat. Anim. Health* **1**: 108–118.
  25. McGurk, C., Morris, D.J., Auchinachie, N.A. and Adams, A. 2006. Development of *Tetracapsuloides bryosalmonae* (Myxozoa:Malacosporea) in bryozoan hosts (as examined by light microscopy) and quantitation of infective dose to rainbow trout (*Oncorhynchus mykiss*). *Vet. Parasitol.* **135**: 249–257.
  26. Molnár, K., Marton, S., Székely, C. and Eszterbauer, E. (2010): Differentiation of *Myxobolus* spp. (Myxozoa: Myxobolidae) infecting roach (*Rutilus rutilus*) in Hungary. *Parasitol Res.* **107**:1137-1150.
  27. Morris, D.J., Terry, R.S., Ferguson, K.D., Smith, J. and Adams, A. 2005. Molecular and ultrastructural characterisation of *Bacillidium vesiculiformis* sp. n. (Microspora: Mrazekiidae) in the freshwater Oligochaete *Nais simplex* (Oligochaeta: Naididae). *Parasitology* **130**: 31–40.
  28. Morris, D.J., Adams, A., Feist, S.W., McGeorge, J. and Richards, R.H. 2000. In situ hybridization identifies the gill as a portal of entry for PKX (Phylum Myxozoa), the causative agent of proliferative kidney disease on salmonids. *Parasit. Res.* **86**: 950-956.
  29. Okamura, B. and Wood, T.S. 2002. Bryozoans as hosts for *Tetracapsula bryosalmonae*, the PKX organism. *J. Fish Dis.* **25**: 469–475.
  30. Saulnier, D., Philippe, H. and De Kinkelin, P. 1999. Molecular evidence that the proliferative kidney disease organism unknown (PKX) is a myxosporean. *Dis. Aquat. Org.* **36**: 209–212.
  31. Schmidt-Posthaus, H., Bettge, K., Forster, U., Segner, H., Wahli, T. 2012. Kidney pathology and parasite intensity in rainbow trout *Oncorhynchus mykiss* surviving proliferative kidney disease: time course and influence of temperature. *Dis Aquat Org* **97**: 207-218.
  32. Seagrave, C.P., Bucke, D. and Mderroan. D.J. 1980. Ultrastructure of a haplosporean-like organism: the possible causative agent of proliferative kidney disease in rainbow trout. *J. Fish Biol.* **16**: 453-459.
  33. Sterud, E., Forseth, T., Ugedal, O., Poppe, T.T., Jorgensen, A., Bruheim, T., Fjeldstad H.P. and Mo T.A. 2007. Severe mortality in wild Atlantic salmon *salmo salar* due to proliferative kidney disease (PKD) caused by *Tetracapsuloid bryosalmonae* (Myxozoa). *Dis. Aquat. Org.* **77**: 191-198.
  34. Wahli, T., Bernet, D., Steiner, P.A. and Schmidt-Posthaus, H. 2007. Geographic distribution of *Tetracapsuloides bryosalmonae* infected fish in Swiss rivers: an update. *Aquat. Sci.* **69**: 3–10.

## Identification of causative agents of PKD in fish

35. Whipps, C.M., Adlard, R.D., Bryant, M.S., Lester, R.J.G., Findlay, V. and Kent, M.L. 2003. First Report of Three Kudoa Species from Eastern Australia: *Kudoa thyrsites* from Mahi mahi (*Coryphaena hippurus*), *Kudoa amamiensis* and *Kudoa minithyrsites* n. sp. from Sweeper (*Pempheris ypsilychnus*). *J. Eukaryot. Microbiol.* **50**: 215-219.
36. Woo, P.T.K. 2006. Myxozoa. In: Fish Diseases and Disorders, Volume 1: Protozoan and Metazoan Infections, 2nd edition (Woo, P.T.K. (ed.), CABI, Oxfordshire, U.K. Pp. 230.
37. Wood, T.S. 2002. Freshwater bryozoans: a zoogeographical reassessment. In: Bryozoan studies 2001 (ed. P. N. Wyse Jackson, C. J. Buttler & M. E. Spencer Jones). Lisse, Netherlands: A. A. Balkema. Pp. 339–345.



التعرف على مسببات مرض الكلى التكاثرى فى أسماك البلطى النيلي وأسماك القظ الأفريقي باستخدام تفاعل

البلمرة المتسلسل مع الإشارة الى التغيرات النسجومرضية المصاحبة

إيمان ابراهيم محمد سرور<sup>1</sup>، كريمة فتحى محروس<sup>2</sup>، اسماعيل عبدالمنعم عيسى<sup>1</sup>،

أمانى عبدالرحمن عباس<sup>1</sup>، عزيزة محمود حسن<sup>2</sup>

<sup>1</sup>قسم أمراض الأسماك ورعايتها - كلية الطب البيطرى - جامعة بنها، <sup>2</sup>قسم بيولوجيا الخلية - المركز القومى للبحوث،

<sup>3</sup>قسم أمراض الأسماك ورعايتها - كلية الطب البيطرى - جامعة قناة السويس

### الملخص العربى

في هذه الدراسة تم التعرف على مسببات مرض الكلى التكاثرى (PKD) في البلطي النيلي وأسماك القظ على أساس حجم وشكل الجراثيم والكبسولات القطبية. داخل هذه الجراثيم. تم التأكد من وجود جراثيم مختلفة من myxosporean عن طريق تقنية البيولوجية الجزيئية بجهاز PCR حيث تم استخدام بريمير عام وخاص لكل نوع. كما تم فحص الانسجة الكلوية من خلال شرائح مصبوعة بالهيماتوكسيلين والايوسين. بعد الفحص الظاهرى بالميكروسكوب للاطوار الناضجة وبعد قياس ابعادها (الطول والعرض) وكذلك أبعاد الاجسام القطبية الداخلية بهذه الاطوار تبين وجود عدد 21 نوع من هذه الاطوار تنتمى الى *Triangula*, *myxobolus*, *Chloromyxum*, *Myxidium*. أظهرت نتائج تفاعل البلمرة المتسلسل فى عينات البلطى النيلي وأسماك القظ الإفريقي عن وجود دلالات تاكد تواجد myxozoa عند 1700 bp وتم التأكد من وجود myxosporea بالتفاعل المتداخل عند 900 bp باستخدام البريمير الخاص بها. كما ظهرت دلالات ال *myxobolus* عند 2000 bp و التفاعل المتداخل عند 1600 bp. كما ظهرت دلالات ال *sphaerospora* عند 1400 bp و دلالات *tetracapsuloid* عند 450 bp. أظهر الفحص الهستوباثولوجى وجود التهاب مزمن فى الكلى المصابة مع تواجد الطفيل السبب للمرض بين الانسجة محاطا بعدد كبير من خلايا *macrophages* و *lymphocyte* مع تناقص ملحوظ فى اعداد الالاناييب الكلوية. كما حدث ضمور وفجوات فى الخلايا المبطننة للاناييب الكلوية مع زيادة وجود النسيج الضام الليفي.

(مجلة بنها للعلوم الطبية البيطرية: عدد 23 (1)، يونيو 2012: 159-170)